Tracer diffusion in hard-sphere colloidal suspensions

Stephen Peppin, *Mississauga, Ontario, Canada*

July 25, 2017

A theory of tracer diffusion in hard-sphere suspensions is developed by using irreversible thermodynamics to obtain a colloidal version of the Kedem-Katchalsky equations. Onsager reciprocity yields relationships between the cross diffusion coefficients of the particles and the reflection coefficient of the colloidal suspension. The theory is illustrated by modelling a self-forming colloidal membrane that filters tracer impurities from the pore fluid.

1. Introduction

Diffusion of tracer particles in colloidal systems occurs in many natural and technological settings including cells and tissues, polymer solutions, soils, water purification systems, biofilms, drug delivery devices, waste containment barriers and microfluidics systems [1]. In contrast to normal diffusion of tracer particles in liquids, colloidal systems often involve coupled effects or membrane phenomena, in which the colloidal particles affect the movement of the tracer particles and vice versa [2, 3, 4]. Owing to the coupling effects, unexpected behaviour can occur such as uphill diffusion [5], the development of anomalous pressures [6] and nonGaussian diffusion [7]. Modelling such systems is challenging owing to a multiplicity of competing effects. In this work a model of a relatively simple case is developed in which the colloidal medium is a hard-sphere suspension

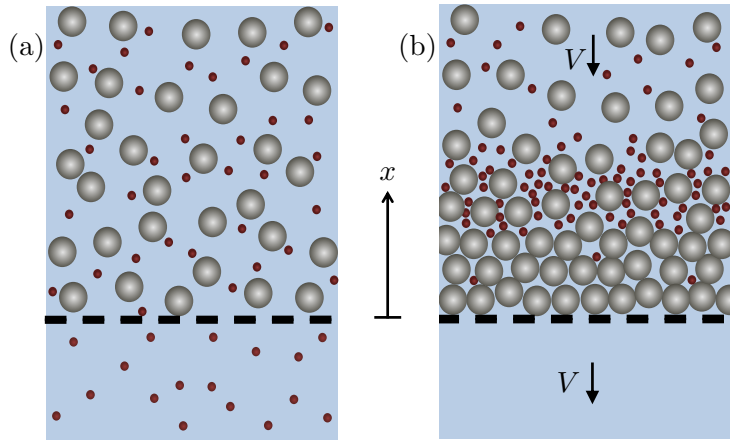

Figure 1: *Schematic of a self-forming dynamic colloidal membrane [8]. (a) A suspension of colloidal particles (grey) and tracer particles (red) is placed above a membrane. The membrane is impermeable to the colloidal particles, but permeable to the tracer particles. (b) A flow $\boldsymbol{v} = -V\hat{\boldsymbol{x}}$ is imposed, consolidating the colloidal particles against the membrane, and forming a dynamic secondary colloidal membrane that traps the tracer particles.*

containing tracer particles in the pore fluid. The results are applied to a water purification system (figure 1) in which the colloidal particles form a dynamic membrane that filters the tracer particles from the pore fluid yielding purified water as the filtrate [8].

In section 2 the equations describing coupled diffusion in colloidal suspensions are presented, and in section 3 the equations are written in a porous media framework leading to a colloidal version of the Kedem-Katchalsky equations. Onsager reciprocity then gives relations between the cross diffusion coefficients and the reflection coefficient σ. Expressions for the dependence of the various coefficients on the volume fraction of colloidal particles are obtained using hydrodynamic models of hindered transport. In section 4 the governing equations are solved for the colloid and tracer particle concentration profiles in an ultrafiltration system. The colloidal particles form a dynamic membrane that filters the tracer particles from the pore fluid.

2. Diffusion and cross-diffusion in colloidal suspensions

From irreversible thermodynamics the flux equations describing cross-diffusion in colloidal suspensions can be written as (see appendix A)

$$\boldsymbol{J}_p = -D_p \boldsymbol{\nabla}\Phi - \Phi D_{dp} \boldsymbol{\nabla}\varphi, \tag{1}$$

$$\boldsymbol{J}_s = -\varphi D_{cd} \boldsymbol{\nabla}\Phi - D_s \boldsymbol{\nabla}\varphi, \tag{2}$$

where Φ is the volume fraction of the large colloidal particles and φ is the volume fraction of the small tracer particles (volume of particles per unit volume of mixture). The flux of colloidal particles is $\boldsymbol{J}_p = \Phi(\boldsymbol{v}_p - \boldsymbol{v})$, where $\boldsymbol{v}_p$ is the average particle velocity and $\boldsymbol{v}$ is the volume average velocity of the mixture. The tracer particle flux is $\boldsymbol{J}_s = \varphi(\boldsymbol{v}_s - \boldsymbol{v})$ and the volume velocity is $\boldsymbol{v} = \Phi\boldsymbol{v}_p + \varphi\boldsymbol{v}_s + \omega\boldsymbol{v}_w$, where $\omega = 1 - \Phi - \varphi$ is the volume fraction of the suspending fluid.

The mutual or collective diffusion coefficient of the colloidal particles is D_p. In binary systems containing only the solvent and colloidal particles, D_p is determined by the generalized Stokes-Einstein equation

$$D_p = \Phi \frac{k}{\mu} \left(\frac{\partial \Pi}{\partial \Phi} \right)_{T,P}, \tag{3}$$

where μ is the viscosity of the pore fluid, k is the permeability of the suspension and Π is the colloid osmotic pressure [9, 10]. Diffusiophoresis modifies equation (3) (*Cf.* Section 3), though the effect is small for dilute tracer concentrations. In (2) D_s is the tracer diffusivity,

$$D_s = \tau D_{s_0}, \tag{4}$$

where $D_{s_0} = k_B T/(6\pi R_s \mu)$ is the Stokes-Einstein diffusivity of the tracer (k_B is Boltzmann's constant, T is temperature and R_s is the radius of the tracer particles) and τ is the diffusive tortuosity factor. Tracer diffusion is hindered ($\tau < 1$) in comparison to that in the pure suspending fluid because the tracer particles diffuse in the restricted and convoluted pore space between the larger colloidal particles. As will be seen in Section 3.2.2, similar to self diffusion in concentrated suspensions [11] as the effective pore radius r_p approaches the size R_s of the tracer particles, $\tau \to 0$ and diffusion is effectively stopped by the presence of the colloidal particles.

The quantity D_{dp} in (1) is the *diffusiophoresis* coefficient characterizing motion of colloidal particles in a gradient of tracer concentration [12]. In a

diffusiophoresis experiment a colloidal particle is placed in a quiescent fluid ($\boldsymbol{v} = 0$) containing a gradient in tracer particle concentration $\boldsymbol{\nabla}\varphi$. The colloidal particle moves owing to a variation in local fluid pressure over the particle surface, set up by the tracer gradient [12]. Equation (1) becomes

$$\boldsymbol{v}_p = -D_{dp}\boldsymbol{\nabla}\varphi \tag{5}$$

so that, given $\boldsymbol{\nabla}\varphi$, a measurement of the particle velocity $\boldsymbol{v}_p$ determines the diffusiophoresis coefficient D_{dp}. For a single colloidal particle surrounded by uncharged hard-sphere tracer particles, calculation of the fluid stress over the particle surface leads to the theoretical relation $D_{dp} = \frac{9}{4}D_{s_0}$ [12, 13].

The *osmotic-diffusion* coefficient D_{cd} in (2) allows for a tracer flux driven by a gradient in colloid particle concentration $\boldsymbol{\nabla}\Phi$ [14]. For a single tracer particle in a quiescent system equation (2) becomes

$$\boldsymbol{v}_s = -D_{cd}\boldsymbol{\nabla}\Phi, \tag{6}$$

so that a measurement of the average tracer velocity $\boldsymbol{v}_s$ yields the osmotic-diffusion coefficient. Experiments obtaining D_{cd} are less common than D_{dp}, though recently Gosting interferometry has obtained D_{cd} for several colloidal systems [15, 14]. In Section 3.1 Onsager reciprocity is used to obtain a relation between D_{cd} and D_{dp}. In Section 3.2 hydrodynamic models of tracer diffusion in pores are used to obtain the dependence of D_{cd} on the colloid volume fraction.

3. Porous media formulation

The flux equations (1) and (2) can be written in a porous media framework by introducing equations of state for the pore pressure p and the tracer osmotic pressure π (figure 2). In general p and π depend on temperature T, mixture pressure P, colloid volume fraction Φ and tracer concentration φ, so that $p = p(T, P, \Phi, \varphi)$ and $\pi = \pi(T, P, \Phi, \varphi)$. In this work T and P are assumed constant. Differentiating π then gives

$$\boldsymbol{\nabla}\pi = \pi_\Phi\boldsymbol{\nabla}\Phi + \pi_\varphi\boldsymbol{\nabla}\varphi, \tag{7}$$

where $\pi_\Phi = (\partial\pi/\partial\Phi)_{T,P,\varphi}$ and $\pi_\varphi = (\partial\pi/\partial\varphi)_{T,P,\Phi}$. Similarly differentiating p yields

$$\boldsymbol{\nabla}p = -\Pi_\Phi\boldsymbol{\nabla}\Phi - \Pi_\varphi\boldsymbol{\nabla}\varphi, \tag{8}$$

where $\Pi_\Phi = (\partial\Pi/\partial\Phi)_{T,P,\varphi}$, $\Pi_\varphi = (\partial\Pi/\partial\varphi)_{T,P,\Phi}$ and the colloid osmotic pressure is the difference between the mixture and pore pressures, $\Pi \equiv P - p$.

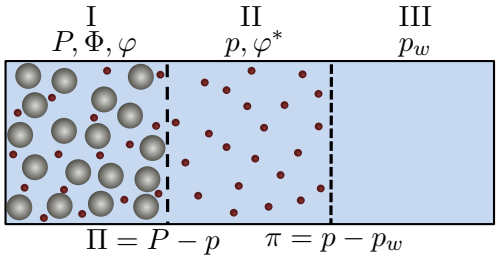

Figure 2: *Illustration of osmotic equilibrium in a colloidal suspension containing tracer particles in the pore fluid. P is the pressure on the full suspension in compartment I, p the pressure on compartment II containing the pore fluid and tracer particles, and p_w the pressure on the pure fluid in III. The membrane separating compartment I from II is permeable to the fluid (blue) and tracer particles (red) but impermeable to the colloidal particles. The difference between the pressures in the two compartments is the colloid osmotic pressure $\Pi \equiv P - p$. The membrane separating compartments II and III is permeable to the fluid but impermeable to the tracer particles. The difference between the pressures in II and III is the tracer osmotic pressure $\pi \equiv p - p_w$. Owing to volume exclusion, the tracer particle volume fraction φ in compartment I is less than the volume fraction φ^* in II. In the absence of depletion effects (dilute tracer concentrations) $\varphi = n\varphi^*$ [16].*

In the infinitely dilute tracer limit $\varphi \to 0$ the colloid osmotic pressure Π is independent of φ [16] so that (8) becomes

$$\boldsymbol{\nabla} p = -\Pi_\Phi \boldsymbol{\nabla} \Phi. \tag{9}$$

The osmotic pressure of the tracer particles is

$$\pi = \frac{\varphi^* k_B T}{\nu_s}, \tag{10}$$

where $\nu_s = \frac{4}{3}\pi R_s^3$ is the tracer particle volume and $\varphi^* = \varphi/n$ is the volume of tracer particles per unit volume of pore space [16] (figure 2). When the tracer concentration is non-dilute the osmotic pressures can be obtained, for example, from multisolute osmotic pressure equations [17, 16].

Inserting (9) and (7) into equations (1) and (2) leads to

$$\boldsymbol{q} = -\frac{k}{\mu}(\boldsymbol{\nabla} p - \sigma_p \boldsymbol{\nabla} \pi), \tag{11}$$

$$\boldsymbol{J}_D = \sigma_d \frac{k}{\mu} \boldsymbol{\nabla} p - \frac{\mathcal{D}_s}{\varphi \pi_\varphi} \boldsymbol{\nabla} \pi, \tag{12}$$

where $\boldsymbol{q} = n(\boldsymbol{v}_f - \boldsymbol{v}_p) = -\boldsymbol{J}_p/\Phi$ is the flux of fluid and tracer particles relative to the colloidal particles, $n = 1-\Phi$ is the porosity (void fraction) of the colloidal particle matrix, $\boldsymbol{J}_D = n\boldsymbol{J}_s/\varphi + \boldsymbol{J}_p = n(\boldsymbol{v}_s - \boldsymbol{v}_f)$ is the tracer particle flux relative to $\boldsymbol{v}_f$, and $\boldsymbol{v}_f = (\varphi\boldsymbol{v}_s + \omega\boldsymbol{v}_w)/n = (\boldsymbol{v} - \Phi\boldsymbol{v}_p)/n$ is the volume velocity of the fluid and tracer particles in the pore space. The permeability k in (11) is

$$\frac{k}{\mu} \equiv -\frac{\boldsymbol{\nabla} p}{\boldsymbol{q}}|_{\boldsymbol{\nabla}\pi=0} = \frac{D_p}{\Phi\Pi_\Phi} - \frac{\varphi D_{dp}}{n\Pi_\Phi}. \tag{13}$$

Solving (13) for D_p leads to a modification of the generalized Stokes-Einstein equation (3) of the form

$$D_p = \Phi\frac{k}{\mu}\Pi_\Phi + \frac{\Phi\varphi}{n}D_{dp}. \tag{14}$$

Thus a positive value of the diffusiophoresis coefficient D_{dp} acts to enhance mutual diffusion of the colloidal particles. For the dilute solute concentrations ($\varphi \sim 10^{-5}$) considered here, however, the second term on the right-hand-side of (14) is negligible so that (14) is equivalent to (3).

The reflection coefficient σ_p in (11) is

$$\sigma_p = \frac{\mu}{k}\frac{D_{dp}}{\pi_\varphi}, \tag{15}$$

and the corresponding coefficient in (12) is

$$\sigma_d = \frac{\mu}{k\Pi_\Phi}\left(nD_{cd} + D_p - \frac{\pi_\Phi}{\pi_\varphi}(nD_s/\varphi - \Phi D_{dp})\right). \tag{16}$$

Finally, the effective diffusivity $\mathcal{D}_s$ in (12) is

$$\mathcal{D}_s = D_s + \Phi\varphi D_{dp}/n. \tag{17}$$

3.1. Kedem Katchalsky equations

Equations (11) and (12) are in the form of *Kedem-Katchalsky* equations,

$$\boldsymbol{q} = -L_P\boldsymbol{\nabla} p - L_{PD}\boldsymbol{\nabla}\pi, \tag{18}$$

$$\boldsymbol{J}_D = -L_{DP}\boldsymbol{\nabla} p - L_D\boldsymbol{\nabla}\pi, \tag{19}$$

where

$$L_p = \frac{k}{\mu}, \quad L_{PD} = \sigma_p\frac{k}{\mu}, \quad L_{DP} = \sigma_d\frac{k}{\mu}, \quad L_D = \frac{\mathcal{D}_s}{\varphi\pi_\varphi} \tag{20}$$

are Onsager transport coefficients and Onsager reciprocity implies $L_{PD} = L_{DP}$ [18, 19] (Appendix A.3). Equation (20) then yields

$$\sigma_p = \sigma_d = \sigma. \tag{21}$$

With (21) equation (15) yields a relation between the diffusiophoresis coefficient and the reflection coefficient

$$D_{dp} = \sigma \frac{k}{\mu} \pi_\varphi. \tag{22}$$

Inserting (15) and (16) into (21) yields an Onsager relation between the cross diffusion coefficients:

$$nD_{cd} = \left(\frac{n\pi_\Phi}{\varphi \pi_\varphi} \right) D_s - D_p + D_{dp} \left(\frac{\Pi_\Phi - \Phi \pi_\Phi}{\pi_\varphi} \right). \tag{23}$$

In the following section hydrodynamic models of the reflection coefficient σ and tortuosity τ for the case of hard spherical particles are used along with the Onsager relation (23) to obtain the volume fraction dependence of the cross diffusion coefficients.

3.2. Volume fraction dependence

3.2.1. Permeability and osmotic pressure

For sufficiently dilute tracer concentrations ($\varphi \to 0$), the permeability and osmotic pressure of a bidisperse suspension depend only on the volume fraction Φ of the larger particles [16, 25]. The permeability can then be written in the form

$$k = \frac{2R^2}{9\Phi} K(\Phi), \tag{24}$$

where K is a dimensionless hindrance factor [9]. For hard-sphere suspensions a Richardson-Zaki type equation

$$K = (1 - \Phi)^\alpha, \tag{25}$$

where $\alpha = 6.55 - 2.5\Phi$, matches experimental data well (figure 3a), agrees with Batchelor's result $K = 1 - 6.55\,\Phi$ in the dilute limit [26] and with the Kozeny-Carman equation $K = (1 - \Phi)^3/10\Phi$ at high colloid concentrations [21].

The colloid osmotic pressure can be written as

$$\Pi = \frac{\Phi k_B T}{\nu_p} Z(\Phi), \tag{26}$$

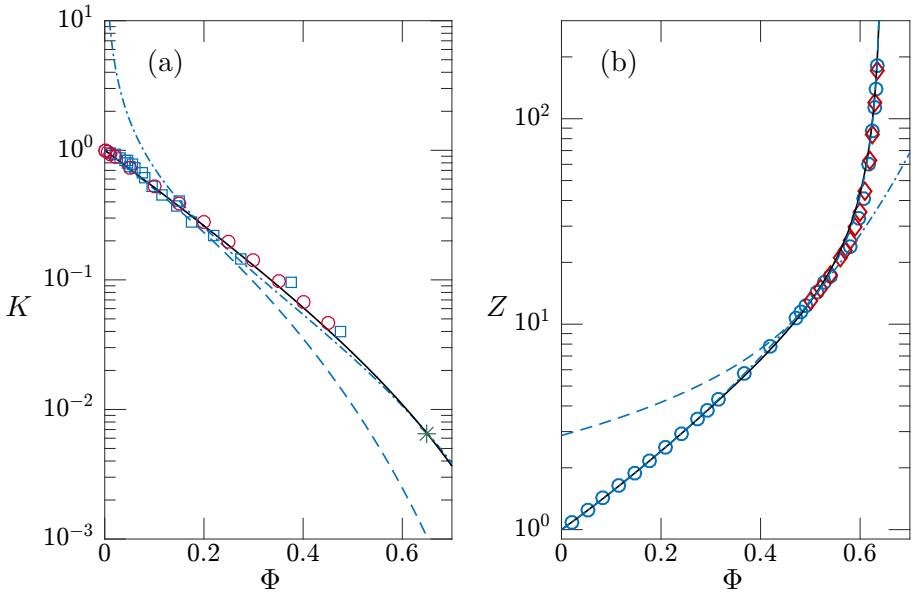

Figure 3: *Plots of (a) hindrance function K and (b) compressibility factor Z as functions of the colloid volume fraction Φ. In (a) the data are from sedimentation experiments (squares) [20], permeation experiments (star) [21], and numerical simulations (circles) [22]. The curves are from equation (25) with $\alpha = 6.55 - 2.5\Phi$ (solid), equation (25) with $\alpha = 6.55$ (dashed), and the Kozeny-Carman equation $K = (1-\Phi)/10\Phi^3$ (dash-dot). In (b) the data are from the molecular dynamics simulations of Wu & Sadus [23] (circles) and Rintoul & Torquato [24] (diamonds). The curves are from equation (27) (solid), the Carnahan-Starling equation of state $Z = (1+\Phi+\Phi^2-\Phi^3)/(1-\Phi)^3$ (dash-dot) and the Woodcock equation of state $Z = 2.89/(1-\Phi/\Phi_p)$ (dash).*

where $\nu_p = \frac{4}{3}\pi R_p^3$ is the volume of a colloidal particle of radius R_p and $Z(\Phi)$ is the compressibility factor [9]. For hard spheres the following expression gives a good fit to molecular dynamics simulations (figure 3b)

$$Z = \frac{1 + a_1\Phi + a_2\Phi^2 + a_3\Phi^3 + a_4\Phi^4}{1 - \Phi/\Phi_p}, \tag{27}$$

where $a_1 = 2.44$, $a_2 = 3.75$, $a_3 = 6.25$, $a_4 = -17$ (Appendix B) and $\Phi_p = 0.64$ is the maximum random close packing fraction [27]. Equation (27) agrees with the Carnahan-Starling equation $Z = (1 + \Phi + \Phi^2 - \Phi^3)/(1 - \Phi)^3$ for $0 < \Phi < 0.5$ and with Woodcock's asymptotic equation of state $Z = 2.89/(1 - \Phi/\Phi_p)$ as $\Phi \to \Phi_p$ [9].

3.2.2. Reflection coefficient and tortuosity

An expression for the dependence of the reflection coefficient σ on porosity for hard-sphere tracer particles in cylindrical pores was derived by Anderson & Quinn [28] in the form

$$\sigma = 1 - (1 - \lambda)^2 K_c, \tag{28}$$

where $K_c = (1 + 2\lambda - \lambda^2)(1 - \frac{2}{3}\lambda^2 - 0.163\lambda^3)$ is a hydrodynamic factor and $\lambda = R_s/r_p$ is the ratio of tracer particle radius R_s to the pore radius r_p.

Equation (28) can be applied to colloidal suspensions by noting that the effective pore size (hydraulic radius) r_p in a suspension is related to the void fraction $n = 1 - \Phi$ via the relation $r_p = n/s_p(1 - n)$ where $s_p = 3/R_p$ is the specific surface area [29] so that

$$\lambda = q_r \frac{3\Phi}{1 - \Phi}, \tag{29}$$

where $q_r = R_s/R_p$ is the ratio of particle sizes.

The tortuosity factor τ can be obtained as a function of λ via the Renkin equation [28]

$$\tau = (1 - \lambda)^2 K_d, \tag{30}$$

where $K_d = 1 - 2.1\lambda + 2.09\lambda^3 - 0.95\lambda^5$. Note that equations (28) and (30) apply when the tracer particles are smaller than the pore radius ($\lambda < 1$). When $\lambda \geq 1$, $\sigma = 1$ and $\tau = 0$ since the particles are in this case larger than the pores. The tortuosity $\tau(\Phi)$ and reflection coefficient $\sigma(\Phi)$ are plotted on figure 4 along with experimental data for τ. At low colloidal particle concentrations ($\Phi \to 0$) the effective pore size is large ($r_p \gg R_s$) and the colloidal particles have little effect on the tracer particles, so that $\sigma \approx 0$ and $\tau \approx 1$. At higher concentrations, however, the pore radius can become equal to or smaller than the tracer particle

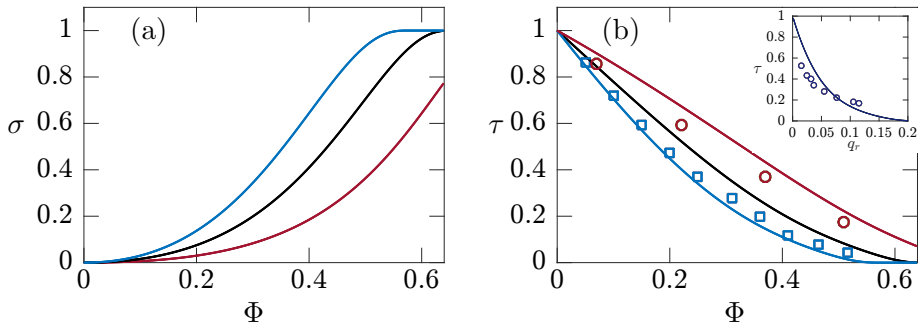

Figure 4: *Plots of (a) the membrane reflection coefficient σ and (b) the diffusive tortuosity τ as functions of the colloid volume fraction Φ for different values of the size ratio $q_r = R_s/R_p$ (blue $q_r = 0.25$, black $q_r = 0.18$, and red $q_r = 0.11$). The data in (b) are from the Brownian dynamics simulations of Kim & Torquato [30] for $q_r = 0.25$ (squares) and $q_r = 0.11$ (circles). The inset to (b) shows τ versus q_r for the case $\Phi = 0.6$, along with experimental data (circles) from Kluijtmans & Philipse [31].*

radius, so that in this limit the colloidal particles significantly hinder the solute particles, and $\tau \to 0$ while $\sigma \to 1$.

3.2.3. Diffusion and cross diffusion coefficients

With these expressions the diffusiophoresis coefficient $D_{dp}(\Phi)$ can be obtained from equation (22), with (28) for σ, (24) for k and (10) for $\pi_\varphi = k_B T/n\nu_s$. For dilute tracer concentrations the viscosity μ of the pore fluid is equal to that of the pure suspending fluid. Equation (14) then gives the colloid diffusion coefficient $D_p(\Phi)$, with Π_Φ obtained by differentiating (26), while (4) combined with (30) gives the solute diffusivity $D_s(\Phi)$. Finally, the osmotic diffusion coefficient $D_{cd}(\Phi)$ is determined by the Onsager relation (23). The diffusion and cross-diffusion coefficients are plotted on figure 5 as functions of Φ for the case $R_p = 1\,\mu$m and $R_s = 0.18\,\mu$m.

The behaviour of D_p (figure 5a) is similar to that observed in previous works on diffusion in hard-sphere suspensions [9, 32]. The slope of the diffusivity curve is reduced at intermediate Φ owing to viscous drag but eventually diverges as $\Phi \to \Phi_p$ owing to volume exclusion [9]. The tracer diffusivity $D_s(\Phi)$ (figure 5d) decreases monotonically with Φ owing to the effects of hindered diffusion, and approaches zero as $\Phi \to \Phi_p$ [30]. The diffusiophoresis coefficient D_{dp}, being proportional to σ, at first increases with Φ (figure 5c). Viscous drag, represented by the permeability $k(\Phi)$, eventually reduces the value of D_{dp} as

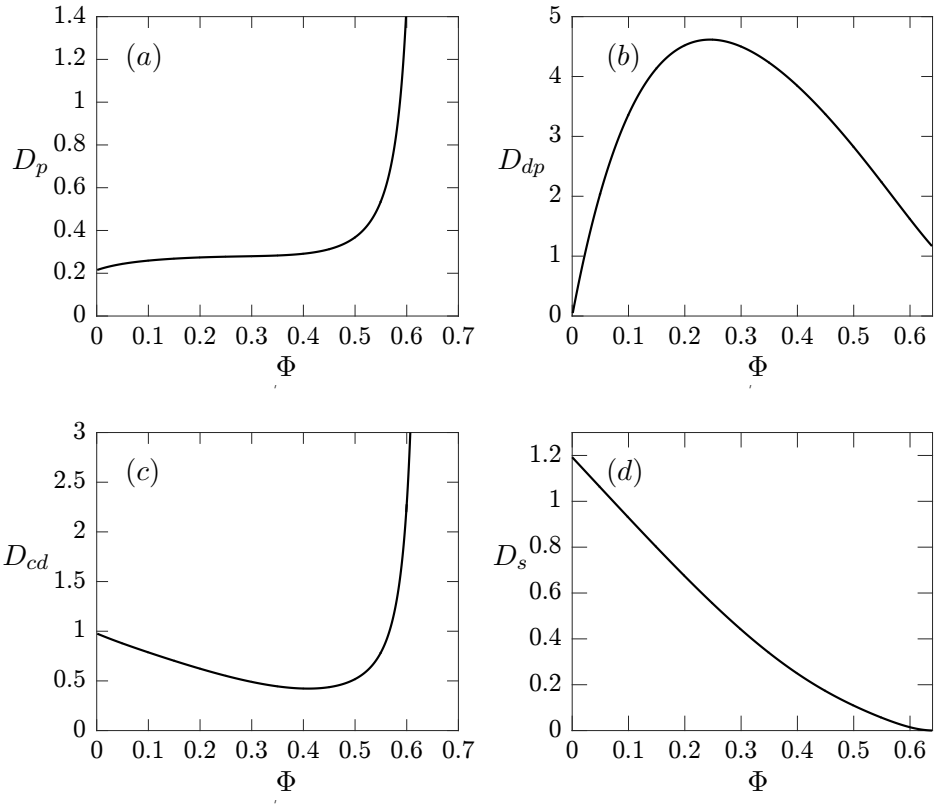

Figure 5: *Plots of the diffusion and cross-diffusion coefficients (in units of $\mu m^2/s$) of the colloidal and tracer particles as functions of colloid volume fraction Φ for the case $\varphi = 10^{-5}$, $R_p = 1\,\mu m$ and $R_s = .18\,\mu m$: (a) mutual diffusion coefficient $D_p(\Phi)$ of the colloidal particles; (b) diffusiophoresis coefficient $D_{dp}(\Phi)$; (c) osmotic diffusion coeffient $D_{cd}(\Phi)$ of the tracer particles; (d) tracer diffusion coefficient $D_s(\Phi)$.*

$\Phi \to \Phi_p$. The behaviour of the cross diffusion coefficient D_{cd} is remarkable, in that it begins as a decreasing function of Φ, but eventually increases and, similarly to D_p, diverges as close packing is approached. This behaviour is owing to the competing terms in the Onsager relation (23). For the infinitely dilute tracer limit ($\varphi \to 0$) and tracer osmotic pressure given by (10), equation (23) takes the simpler form (using also equations (22) and (14))

$$nD_{cd} = D_s - D_p(1 - \sigma/\Phi). \tag{31}$$

In the limit of a perfect membrane ($\sigma \to 1$ and $D_s \to 0$) equation (31) gives $D_{cd} = D_p/\Phi$, while in the dilute colloid limit ($\Phi \to 0$ and $\sigma \to 0$) equation (31) gives $D_{cd} = D_s - D_p$. If in addition $q_r \ll 1$ (tracer particles much smaller than colloidal particles), $D_{cd} = D_s$. (With equation (56) this becomes $D_{21} = C_1\bar{V}_1 D_{22}$, in agreement with Annunziata [2] and Bruna & Chapman [33].) Thus D_{cd} represents a competition between the tracer diffusivity D_s at low Φ and the colloid diffusivity D_p at high Φ. As will be seen in the next section, the rapid increase of D_{cd} as $\Phi \to \Phi_p$ allows the colloidal suspension to behave like a separation membrane that actively prohibits the tracer particles from passing through.

4. Application to ultrafiltration

In ultrafiltration systems a colloidal suspension is advected toward a membrane or porous support that is impermeable to the colloidal particles, but through which the pore fluid and tracer particles can pass (figure 1). Ultrafiltration is used extensively in industry to purify water, process pharmaceuticals and concentrate milk and juices [34]. During the filtration process the colloidal particles build up adjacent to the membrane forming a concentration polarization layer. The large colloid osmotic pressure in this layer can lead to detrimental effects such as membrane fouling and flux decline [35]. On the other hand if the colloidal particles exhibit membrane properties, the concentration polarization layer itself becomes a secondary dynamic filtration membrane that can be used to remove tracer particles from the pore fluid. Recent experimental studies demonstrate the excellent potential of dynamic colloidal membranes for water purification applications [8]. The membranes form naturally, are relatively inexpensive to produce and can be easily removed and regenerated, mitigating the effects of membrane fouling. A significant advantage of such systems is that expensive ultrafiltration membranes are not required, since the secondary dynamic membrane performs the filtration. Recently, CO_2 injection has been

used in place of the porous support, creating the possibility of completely membrane-free water purification [36].

Figure 1 shows a schematic of the system to be studied. At $x = 0$ is a porous support or mesh that is permeable to the fluid and tracer particles, but impermeable to the colloidal particles. Above the support is a colloidal suspension of initial volume fraction Φ_0 containing tracer particles at φ_0. At $t = 0$ a volume flow $\boldsymbol{v} = -V\hat{\boldsymbol{x}}$ is imposed and the colloidal particles are advected toward the porous support, forming a concentration polarization layer.

4.1. Governing equations

For the one-dimensional system in figure 1, conservation of mass can be written as (appendix C)

$$\frac{\partial \Phi}{\partial t} - V\frac{\partial \Phi}{\partial x} = -\frac{\partial J_p}{\partial x} \qquad (x > 0), \tag{32}$$

$$\frac{\partial \varphi}{\partial t} - V\frac{\partial \varphi}{\partial x} = -\frac{\partial J_s}{\partial x} \qquad (x > 0), \tag{33}$$

where the fluxes are

$$J_p = -D_p\frac{\partial \Phi}{\partial x} - \Phi D_{dp}\frac{\partial \varphi}{\partial x}, \tag{34}$$

and

$$J_s = -\varphi D_{cd}\frac{\partial \Phi}{\partial x} - D_s\frac{\partial \varphi}{\partial x}. \tag{35}$$

4.1.1. Initial and boundary conditions

Initially there is a semi-infinite layer of colloidal suspension above the porous support, of uniform concentration so that

$$\Phi = \Phi_0 \quad \text{and} \quad \varphi = \varphi_0 \qquad (0 \le x < \infty). \tag{36}$$

The boundary conditions are that the membrane support at $x = 0$ is impermeable to the colloidal particles: ($\boldsymbol{v}_p = 0$) and permeable to the tracer particles: ($\boldsymbol{v}_s = \boldsymbol{v}$). With these conditions the fluxes at $x = 0$ become $\boldsymbol{J}_p = -\Phi\boldsymbol{v} = \Phi V\hat{\boldsymbol{x}}$ and $\boldsymbol{J}_s = 0$, and equations (34) and (35) then give the boundary conditions at the porous support as

$$\Phi V = -D_p\frac{\partial \Phi}{\partial x} - \Phi D_{dp}\frac{\partial \varphi}{\partial x} \qquad (x = 0), \tag{37}$$

$$0 = -\varphi D_{cd}\frac{\partial \Phi}{\partial x} - D_s\frac{\partial \varphi}{\partial x} \qquad (x = 0). \tag{38}$$

The far field boundary conditions are that

$$\Phi \to \Phi_0 \quad \text{and} \quad \varphi \to \varphi_0 \qquad (x \to \infty). \tag{39}$$

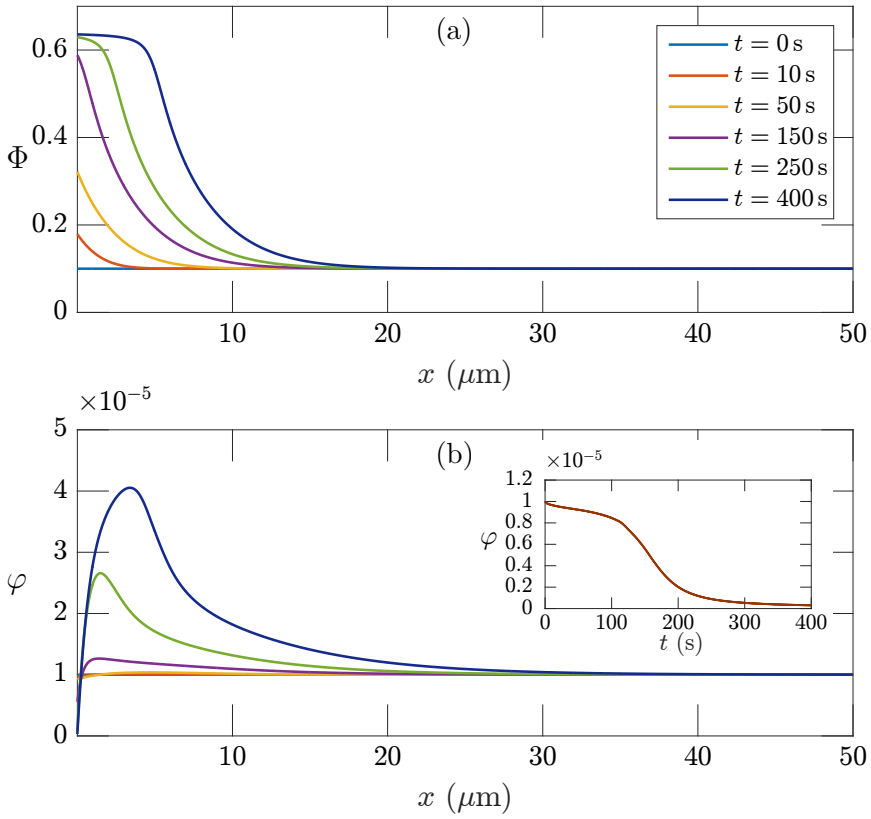

Figure 6: *(a) Colloid volume fraction $\Phi(x,t)$ and (b) tracer concentration $\varphi(x,t)$ profiles obtained by solving equations (32)–(39). The inset to (b) shows the time evolution of the tracer particle concentration entering the filtrate at $x = 0$.*

4.2. Results

Equations (32)–(39) were solved using the MATLAB partial differential equation solver pdepe for the case $\{\Phi_0 = 0.1,\ \varphi_0 = 10^{-5},\ R_p = 1\,\mu\mathrm{m},\ R_s = 0.18\,\mu\mathrm{m}$ and $V = 0.1\,\mu\mathrm{m/s}\}$. The results for $\Phi(x,t)$ and $\varphi(x,t)$ are shown in figure 6. At early times ($t = 10\,\mathrm{s}$ and $t = 50\,\mathrm{s}$), the colloid volume fraction increases rapidly against the support at $x = 0$ (figure 6a), but the tracer particle concentration is relatively unchanged from it's initial value φ_0 (figure 6b). The colloidal suspension is still fairly porous at this stage and the tracer particles are able to pass through into the filtrate relatively unhindered. However, as the colloid is further consolidated ($t = 150\,\mathrm{s}$), the volume fraction at $x = 0$ approaches close packing and the tracer particles can no longer easily fit through. The

reflection coefficient σ approaches 1, causing the tracer particles to become trapped. At longer times ($t = 250\,\mathrm{s}$ and $t = 400\,\mathrm{s}$) the colloidal particles almost completely block the tracer particles, and a large tracer polarization layer forms within the colloidal membrane. The inset to figure 6b shows the time evolution of the tracer concentration entering the filtrate at $x = 0$. Once the dynamic membrane has formed ($t > 150\,\mathrm{s}$), the tracer concentration entering the filtrate drops rapidly, approaching zero at longer times.

The membrane effect is caused by the osmotic diffusion D_{cd} term in the tracer flux equation (35). In the ultrafiltration system in figure 6, $\partial\Phi/\partial x < 0$ while $\partial\varphi/\partial x > 0$ at $x = 0$, and therefore the two terms on the right hand side of (35) are of opposite sign. The main D_s diffusion term acts to relax the tracer concentration gradient and move the particles through the membrane in the $-x$ direction, while the osmotic diffusion term is driving them in the positive x direction. When the colloid volume fraction Φ is large, hindered diffusion causes the tracer diffusion coefficient D_s to reduce to near zero (figure 5d). The osmotic diffusion coefficient D_{cd}, however, becomes large in this limit (figure 5c) and prohibits the tracer particles from passing through the membrane.

5. Conclusions

A phenomenological theory of tracer diffusion and membrane effects in colloidal suspensions has been derived. The coupled diffusion equations have been transformed into Kedem-Katchalsky equations, yielding relations between the cross diffusion coefficients and the reflection coefficient of the colloidal membrane. As an example application the equations have been solved for an ultrafiltration system. The colloidal particles form a dynamic membrane that filters the tracer particles from the pore fluid.

A. Non-equilibrium thermodynamics of cross-diffusion

The following derivation is given in detail as it differs in some respects for colloidal suspensions from previous works on discontinuous systems [18, 37], particularly in the treatment of chemical potentials and pressures in section A.3. From irreversible thermodynamics the rate of entropy production Σ in a three-component system at constant temperature T and pressure P is given by the equation [37, 18]

$$-T\Sigma = \boldsymbol{J}_0 \cdot \boldsymbol{\nabla}_{T,P}\mu_0 + \boldsymbol{J}_1 \cdot \boldsymbol{\nabla}_{T,P}\mu_1 + \boldsymbol{J}_2 \cdot \boldsymbol{\nabla}_{T,P}\mu_2 \tag{40}$$

where $\boldsymbol{J}_k = C_k \boldsymbol{v}_k$ is the molar flux of component k moving at velocity $\boldsymbol{v}_k$ and μ_k and C_k are the molar chemical potential and the molar concentration (moles per unit volume of mixture), respectively, of k. Here, component '0' is taken to be the fluid, '1' the colloidal particles and '2' the tracer particles. The subscript T, P denotes the gradient taken with T and P held constant [37],

Equation (40) can be written in terms of independent fluxes and forces using the Gibbs-Duhem equation [37, 18] which states that at constant T and P

$$C_0 \boldsymbol{\nabla}_{T,P} \mu_0 + C_1 \boldsymbol{\nabla}_{T,P} \mu_1 + C_2 \boldsymbol{\nabla}_{T,P} \mu_2 = 0. \tag{41}$$

Inserting (41) into (40) to eliminate $\boldsymbol{\nabla}_{T,P} \mu_0$ leads to

$$-T\Sigma = \boldsymbol{J}_1^0 \cdot \boldsymbol{\nabla}_{T,P} \mu_1 + \boldsymbol{J}_2^0 \cdot \boldsymbol{\nabla}_{T,P} \mu_2, \tag{42}$$

where $\boldsymbol{J}_k^0 = C_k(\boldsymbol{v}_k - \boldsymbol{v}_0)$ is the flux of k relative to the fluid component 0. It is a postulate of linear irreversible thermodynamics [37] that when the entropy production Σ is written as the sum of products of independent fluxes and independent forces, the fluxes can be written as linear functions of the forces such that

$$\boldsymbol{J}_1^0 = -L_{11}^0 \boldsymbol{\nabla}_{T,P} \mu_1 - L_{12}^0 \boldsymbol{\nabla}_{T,P} \mu_2, \tag{43}$$

$$\boldsymbol{J}_2^0 = -L_{21}^0 \boldsymbol{\nabla}_{T,P} \mu_1 - L_{22}^0 \boldsymbol{\nabla}_{T,P} \mu_2, \tag{44}$$

and the matrix of coefficients L_{ik} obeys the Onsager reciprocal relations

$$L_{12}^0 = L_{21}^0.$$

Furthermore, one is free to choose more experimentally convenient forces (such as gradients in concentration) and, so long as the fluxes and forces making up Σ are independent, the coefficient matrix of the flux equations will continue to be symmetric [37]. This result is used below to derive more convenient forms of the flux equations.

For example in experimental systems it is often convenient to define the fluxes relative to the volume-average velocity $\boldsymbol{v}$ rather than the solvent velocity $\boldsymbol{v}_0$ since $\boldsymbol{v} = 0$ or $\boldsymbol{\nabla} \cdot \boldsymbol{v} = 0$ in many systems [37]. The volume average velocity is

$$\boldsymbol{v} = \Phi_0 \boldsymbol{v}_0 + \Phi_1 \boldsymbol{v}_1 + \Phi_2 \boldsymbol{v}_2, \tag{45}$$

where $\Phi_k = C_k \bar{V}_k$ is the volume fraction of k, with $\bar{V}_k$ the partial molar volume. A thermodynamic Euler relation gives $C_0 \bar{V}_0 + C_1 \bar{V}_1 + C_2 \bar{V}_2 = 1$ [37, 38] or in terms of volume fractions

$$\Phi_0 + \Phi_1 + \Phi_2 = 1. \tag{46}$$

With this definition of $\boldsymbol{v}$ one can write $\boldsymbol{J}_k^0 = \boldsymbol{J}_k^v - (C_k/C_0)\boldsymbol{J}_0^v$ where $\boldsymbol{J}_k^v = C_k(\boldsymbol{v}_k - \boldsymbol{v})$ is the flux of k relative to $\boldsymbol{v}$, so that (42) can be written in the equivalent form

$$-T\Sigma = \boldsymbol{J}_1^v \cdot \boldsymbol{\nabla}_{T,P}\tilde{\mu_1} + \boldsymbol{J}_2^v \cdot \boldsymbol{\nabla}_{T,P}\tilde{\mu_2}, \tag{47}$$

where $\tilde{\mu_k} = \mu_k - (\bar{V}_k/\bar{V}_0)\mu_0$. In obtaining (47) the Gibbs-Duhem equation (41) has been used along with the fact that $\bar{V}_0\boldsymbol{J}_0^v + \bar{V}_1\boldsymbol{J}_1^v + \bar{V}_2\boldsymbol{J}_2^v = 0$ (which can be verified using the definition of $\boldsymbol{J}_k^v$ and (46)).

Equation (47) is also a sum of independent fluxes and forces and therefore linear flux equations can be postulated as

$$\boldsymbol{J}_1^v = -L_{11}^v\boldsymbol{\nabla}_{T,P}\tilde{\mu}_1 - L_{12}^v\boldsymbol{\nabla}_{T,P}\tilde{\mu}_2, \tag{48}$$

$$\boldsymbol{J}_2^v = -L_{21}^v\boldsymbol{\nabla}_{T,P}\tilde{\mu}_1 - L_{22}^v\boldsymbol{\nabla}_{T,P}\tilde{\mu}_2, \tag{49}$$

and the Onsager relation is $L_{12}^v = L_{21}^v$.

A.1. Concentration formalism

As it is not often possible to measure chemical potentials directly (though recently this has been achieved via confocal microscopy [39]) the flux equations can be written in terms of gradients in the concentrations C_k [18, 2]. At constant temperature T and mixture pressure P the chemical potentials depend only on C_1 and C_2 and the gradients can be written as $\boldsymbol{\nabla}_{T,P}\tilde{\mu}_k = \tilde{\mu}_{k1}\boldsymbol{\nabla}C_1 + \tilde{\mu}_{k2}\boldsymbol{\nabla}C_2$ where $\tilde{\mu}_{kj} = (\partial\tilde{\mu}_k/\partial C_j)_{T,P,C_i,i\neq j}$. The flux equations (48) and (49) become

$$\boldsymbol{J}_1^v = -D_{11}\boldsymbol{\nabla}C_1 - D_{12}\boldsymbol{\nabla}C_2, \tag{50}$$

$$\boldsymbol{J}_2^v = -D_{21}\boldsymbol{\nabla}C_1 - D_{22}\boldsymbol{\nabla}C_2, \tag{51}$$

where the diffusivities D_{ij} are

$$D_{ij} = \sum_{k=1}^{2} L_{ik}^v\tilde{\mu}_{kj}. \tag{52}$$

A.2. Volume fraction formalism

Alternatively, and more conveniently for the present work, the equations can be written in terms of the gradients of volume fraction $\Phi_k = C_k\bar{V}_k$ of the colloidal particles and the tracer particles. In hard-sphere suspensions the colloidal and tracer partial molar volumes are constants ($1/\bar{V}_k = Na\,\nu_k$, where Na is Avogadro's number and $\nu_k = \frac{4}{3}\pi R_k^3$ is the particle volume), in which case the flux equations (50) and (51) can be written in terms of Φ_1 and Φ_2 to give

$$\boldsymbol{J}_p = -D_p \boldsymbol{\nabla}\Phi_1 - \Phi_1 D_{dp} \boldsymbol{\nabla}\Phi_2, \tag{53}$$

$$\boldsymbol{J}_s = -\Phi_2 D_{cd} \boldsymbol{\nabla}\Phi_1 - D_s \boldsymbol{\nabla}\Phi_2, \tag{54}$$

where $\boldsymbol{J}_p = \Phi_1(\boldsymbol{v}_1 - \boldsymbol{v}) = \boldsymbol{J}_1^v \bar{V}_1$, $\boldsymbol{J}_s = \Phi_2(\boldsymbol{v}_2 - \boldsymbol{v}) = \boldsymbol{J}_2^v \bar{V}_2$ and the diffusion coefficients are

$$D_p = D_{11}, \quad D_{dp} = D_{12}/C_1\bar{V}_2, \tag{55}$$

$$D_{cd} = D_{21}/C_2\bar{V}_1, \quad D_s = D_{22}. \tag{56}$$

Equations (53) and (54) are equivalent to (1) and (2), in which for convenience the symbols Φ, φ, $\boldsymbol{v}_p$ and $\boldsymbol{v}_s$ are used in place of Φ_1, Φ_2, $\boldsymbol{v}_1$ and $\boldsymbol{v}_2$.

A.3. Pore pressure formalism (Kedem-Katchalsky equations)

The entropy production Σ can alternatively be written in terms of the pore pressure P^* (denoted p in figure 2) and osmotic pressure π of the tracer particles in the pore fluid [18]. Starting from equation (40) and using the Gibbs-Duhem equation (41) to eliminate $\boldsymbol{\nabla}_{T,P}\mu_1$ leads to

$$-T\Sigma = \boldsymbol{J}_0^1 \cdot \boldsymbol{\nabla}_{T,P}\mu_0 + \boldsymbol{J}_2^1 \cdot \boldsymbol{\nabla}_{T,P}\mu_2, \tag{57}$$

where $\boldsymbol{J}_k^1 = C_k(\boldsymbol{v}_k - \boldsymbol{v}_1)$ is the flux of k relative to the colloidal particles. In order to replace the chemical potentials μ_0 and μ_2 with the measureable quantities p and π we consider a Darcy permeameter or reservoir that is separated from the suspension by a membrane or partition that is impermeable to the colloidal particles but permeable to the pore fluid and tracer particles (figure 2). Placing permeameters at different locations in the suspension gives profiles of pore pressure [10]. Local equilibrium between the colloidal suspension and the tracer suspension in the permeameter implies equality of the fluid and tracer chemical potentials on each side of the partition so that $\mu_0(T, P, C_1, C_2) = \mu_0^*(T, P^*, C_2^*)$ and $\mu_2(T, P, C_1, C_2) = \mu_2^*(T, P^*, C_2^*)$, where μ_k^* is the chemical potential of k in the permeameter. Assuming there is no adsorption of the tracer particles by the colloidal particles and ignoring depletion effects [16], the tracer and fluid concentrations in the permeameter are

$$C_0^* = C_0/n \qquad C_2^* = C_2/n, \tag{58}$$

where $n = 1 - \Phi_1$ is the porosity [16]. Taking gradients of the chemical potentials gives, at constant temperature T and mixture pressure P (the pore pressure P^* is variable),

$$\boldsymbol{\nabla}_{T,P}\mu_0(T, P, C_1, C_2) = \boldsymbol{\nabla}_T\mu_0^*(P^*, C_2^*) = \boldsymbol{\nabla}_{T,P^*}\mu_0^*(C_2^*) + \bar{V}_0^* \boldsymbol{\nabla} P^*, \tag{59}$$

$$\boldsymbol{\nabla}_{T,P}\mu_2(T,P,C_1,C_2) = \boldsymbol{\nabla}_T\mu_2^D(P^*,C_2^*) = \boldsymbol{\nabla}_{T,P^*}\mu_2^*(C_2^*) + \bar{V}_2^*\boldsymbol{\nabla}P^*, \tag{60}$$

where $\bar{V}_k^* = (\partial\mu_k^*/\partial P^*)_{T,C_2^*}$ is the partial molar volume of k in the permeameter [38]. For hard-sphere tracer particles $\bar{V}_2^* = \bar{V}_2 = Na\nu_2$, where Na is Avogadro's number and ν_2 is the volume of a particle. The Gibbs-Duhem equation applied to the tracer suspension in the permeameter is

$$C_0^*\boldsymbol{\nabla}_{T,P^*}\mu_0^* + C_2^*\boldsymbol{\nabla}_{T,P^*}\mu_2^* = 0. \tag{61}$$

Inserting (59)–(61) into (57) gives

$$-T\Sigma = \left(\boldsymbol{J}_0^1 - \frac{C_0^*}{C_2^*}\boldsymbol{J}_2^1\right)\cdot\boldsymbol{\nabla}_{T,P^*}\mu_0^* + (\bar{V}_0^*\boldsymbol{J}_0^1 + \bar{V}_2^*\boldsymbol{J}_2^1)\cdot\boldsymbol{\nabla}P^*. \tag{62}$$

The chemical potential gradient of the fluid component in the reservoir is

$$\boldsymbol{\nabla}_{T,P^*}\mu_0^* = -V_w\boldsymbol{\nabla}\pi, \tag{63}$$

where V_w is the molar volume of the pure fluid [38]. For inert hard-sphere suspensions $\bar{V}_0 = \bar{V}_0^* = V_w = M_w/\rho_w$, where M_w and ρ_w are the molar mass and density of the pure fluid. With (63) and (58) the entropy production (62) takes the Kedem-Katchalsky form

$$-T\Sigma = \boldsymbol{J}_D\cdot\boldsymbol{\nabla}\pi + \boldsymbol{q}\cdot\boldsymbol{\nabla}P^*, \tag{64}$$

where $\boldsymbol{J}_D = \bar{V}_0^*\left(C_0^*\boldsymbol{J}_2^1/C_2^* - \boldsymbol{J}_0^1\right) = n\Phi_0^*(\boldsymbol{v}_2 - \boldsymbol{v}_0) = n(\boldsymbol{v}_2 - \boldsymbol{v}_f)$ and $\boldsymbol{q} = \bar{V}_0^*\boldsymbol{J}_0^1 + \bar{V}_2^*\boldsymbol{J}_2^1 = n(\boldsymbol{v}_f - \boldsymbol{v}_1)$. The volume-average velocity of the fluid and tracer particles is $\boldsymbol{v}_f = \Phi_0^*\boldsymbol{v}_0 + \Phi_2^*\boldsymbol{v}_2$, where $\Phi_0^* = C_0^*\bar{V}_0^*$ and $\Phi_2^* = C_2^*\bar{V}_2^*$ are the volume fraction of the pore space occupied by the fluid and tracer particles, respectively. The colloidal particles cannot enter the permeameter, so that $\Phi_1^* = 0$ and $\Phi_0^* + \Phi_2^* = 1$.

Since the fluxes and forces in (64) are independent we can postulate linear relations between them giving the Kedem-Katchalsky equations

$$\boldsymbol{q} = -L_P\boldsymbol{\nabla}P^* - L_{PD}\boldsymbol{\nabla}\pi, \tag{65}$$

$$\boldsymbol{J}_D = -L_{DP}\boldsymbol{\nabla}P^* - L_D\boldsymbol{\nabla}\pi, \tag{66}$$

and Onsager reciprocity gives $L_{PD} = L_{DP}$. Equations (65) and (66) are equivalent to (18) and (19), where for convenience the symbol p is used for the pore pressure in place of P^*.

B. Parameter estimation for the hard-sphere EOS

The coefficients a_1 and a_2 in equation (27) were determined by requiring that $Z \to 1 + 4\Phi + 10\Phi^2$ as $\Phi \to 0$ giving $a_1 = 4 - 1/\Phi_p = 2.44$ and $a_2 = 10 - 4/\Phi_p = 3.75$. a_3 was treated as an adjustable parameter to achieve a best fit to the molecular dynamics data for $Z(\Phi)$, yielding $a_3 = 6.25$, and a_4 was determined by requiring that $Z \to 2.89/(1 - \Phi/\Phi_p)$ as $\Phi \to \Phi_p$ giving $a_4 = (1.89 - a_1\Phi_p - a_2\Phi_p^2 - a_3\Phi_p^3)/\Phi_p^4 = -17.0$.

C. Conservation of mass

For a multicomponent system conservation of mass of each species is [29, 37]

$$\frac{\partial \rho_k}{\partial t} + \boldsymbol{\nabla} \cdot \rho_k \boldsymbol{v}_k = 0, \tag{67}$$

where ρ_k is the mass of component k per unit volume of the mixture. For hard-sphere suspensions $\rho_k = \Phi_k m_k/\nu_k$, where m_k and ν_k are the mass and volume per particle, and (67) becomes

$$\frac{\partial \Phi_k}{\partial t} + \boldsymbol{\nabla} \cdot \Phi_k \boldsymbol{v}_k = 0. \tag{68}$$

For relatively slow transport (such that an assumption of local equilibrium applies) it is often the case that volumes are conserved and the volume-average velocity is divergence free, $\boldsymbol{\nabla} \cdot \boldsymbol{v} = 0$ [37]. Using the vector identity $\boldsymbol{\nabla} \cdot \Phi_k \boldsymbol{v} = \boldsymbol{v} \cdot \boldsymbol{\nabla}\Phi_k + \Phi_k \boldsymbol{\nabla} \cdot \boldsymbol{v}$ equation (68) becomes

$$\frac{\partial \Phi_k}{\partial t} + \boldsymbol{v} \cdot \boldsymbol{\nabla}\Phi_k = -\boldsymbol{\nabla} \cdot \boldsymbol{J}_k, \tag{69}$$

where $\boldsymbol{J}_k = \Phi_k(\boldsymbol{v}_k - \boldsymbol{v})$.

References

[1] E. L. Cussler. *Diffusion: Mass Transfer in Fluid Systems*. Cambridge University Press, U.K., 2009.

[2] O. Annunziata. On the role of solute solvation and excluded-volume interactions in coupled diffusion. *The Journal of Physical Chemistry B*, 112(38):11968–11975, 2008.

[3] M. A. Malusis, C. D. Shackelford, and J. E. Maneval. Critical review of coupled flux formulations for clay membranes based on nonequilibrium thermodynamics. *Journal of Contaminant Hydrology*, 138:40 – 59, 2012.

[4] D. Velegol, A. Garg, R. Guha, A. Kar, and M. Kumar. Origins of concentration gradients for diffusiophoresis. *Soft Matter*, 12:4686–4703, 2016.

[5] M. A. Glaus, M. Birgersson, O. Karnland, and L. R. Van Loon. Seeming steady-state uphill diffusion of 22na+ in compacted montmorillonite. *Environmental Science & Technology*, 47(20):11522–11527, 2013.

[6] C. E. Neuzil and A. M. Provost. Recent experimental data may point to a greater role for osmotic pressures in the subsurface. *Water Resources Research*, 45(3):W03410, 2009.

[7] J. Guan, B. Wang, and S. Granick. Even hard-sphere colloidal suspensions display fickian yet non-gaussian diffusion. *ACS Nano*, 8(4):3331–3336, 2014.

[8] M. E. Ersahin, H. Ozgun, R. K. Dereli, I. Ozturk, K. Roest, and J. B.van Lier. A review on dynamic membrane filtration: Materials, applications and future perspectives. *Bioresource Technology*, 122:196–206, 2012.

[9] W. B. Russel, D. A. Seville, and W. R. Schowalter. *Colloidal Dispersions*. Cambridge University Press, U.K., 1989.

[10] S. S. L. Peppin, J. A. W. Elliott, and M. G. Worster. Pressure and relative motion in colloidal suspensions. *Physics of Fluids*, 17(5):053301, 2005.

[11] J. M. Rallison. Brownian diffusion in concentrated suspensions of interacting particles. *Journal of Fluid Mechanics*, 186:471–500, 1988.

[12] J. L. Anderson. Colloid transport by interfacial forces. *Annual Review of Fluid Mechanics*, 21:61–99, 1989.

[13] Staffeld and Quinn. Diffusion-induced banding of colloid particles via diffusiophoresis: 2. non-electrolytes. *Journal of Colloid and Interface Science*, 130:88–100, 1989.

[14] O. Annunziata, D. Buzatu, and J. G. Albright. Protein diffusiophoresis and salt osmotic diffusion in aqueous solutions. *The Journal of Physical Chemistry B*, 116(42):12694–12705, 2012.

[15] A. Vergara, O. Annunziata, L. Paduano, D. G. Miller, J. G. Albright, and R. Sartorio. Multicomponent diffusion in crowded solutions. 2. mutual diffusion in the ternary system tetra(ethylene glycol)naclwater. *The Journal of Physical Chemistry B*, 108(8):2764–2772, 2004.

[16] H. N. W. Lekkerkerker and A. Stroobants. On the spinodal instability of highly asymmetric hard sphere suspensions. *Physica A*, 195:387–397, 1993.

[17] M. W. Zielinski, L. E. McGann, J. A. Nychka, and J. A. W. Elliott. Comparison of non-ideal solution theories for multi-solute solutions in cryobiology and tabulation of required coefficients. *Cryobiology*, 69:305–317, 2014.

[18] A. Katzir-Katchalsky and P. F. Curran. *Nonequilibrium Thermodynamics in Biophysics*. Harvard University Press, Boston, 1965.

[19] J. A. W. Elliott, H. Y. Elmoazzan, and L. E. McGann. A method whereby onsager coefficients may be evaluated. *Journal of Chemical Physics*, 113:6573, 2000.

[20] R. Buscall, J. W. Goodwin, R. H. Ottewill, and Th. F. Tadros. The settling of particles through newtonian and non-newtonian media. *Journal of Colloid and Interface Science*, 85:78–86, 1982.

[21] A. P. Philipse and C. Pathmamanoharan. Liquid permeation (and sedimentation) of dense colloidal hard-sphere packings. *Journal of Colloid and Interface Science*, 159:96–107, 1993.

[22] A. J. C. Ladd. Hydrodynamic transport coefficients of random dispersions of hard spheres. *The Journal of Chemical Physics*, 93:3484–3494, 1990.

[23] G.-W. Wu and R. J. Sadus. Hard sphere compressibility factors for equation of state development. *AIChE Journal*, 51:309–313, 2005.

[24] M. D. Rintoul and S. Torquato. Computer simulations of dense hardsphere systems. *The Journal of Chemical Physics*, 105:9258–9265, 1996.

[25] D. M. E. Thies-Weesie and A. P. Philipse. Liquid permeation of bidisperse colloidal hard-sphere packings and the kozeny-carman scaling relation. *Journal of Colloid and Interface Science*, 162:470–480, 1994.

[26] G. K. Batchelor. Brownian diffusion of particles with hydrodynamic interaction. *Journal of Fluid Mechanics*, 74:1–29, 1976.

[27] R. D. Kamien and A. J. Liu. Why is random close packing reproducible? *Phys. Rev. Lett.*, 99:155501, 2007.

[28] J. L. Anderson and J. A. Quinn. Restricted transport in small pores: A model for steric exclusion and hindered particle motion. *Biophysical Journal*, 14:130–150, 1974.

[29] R. B. Bird, W. E. Stuart, and E. N. Lightfoot. *Transport Phenomena Second Edition*. Wiley, N.Y., 2002.

[30] I. C. Kim and S. Torquato. Diffusion of finitesized brownian particles in porous media. *The Journal of Chemical Physics*, 96(2):1498–1503, 1992.

[31] S. G. J. M. Kluijtmans and A. P. Philipse. First in situ determination of confined brownian tracer motion in dense random sphere packings. *Langmuir*, 15(6):1896–1898, 1999.

[32] S. S. L. Peppin, J. A. W. Elliott, and M. G. Worster. Solidification of colloidal suspensions. *J. Fluid Mech.*, 554:147–166, 2006.

[33] M. Bruna and S. J. Chapman. Diffusion of multiple species with excluded-volume effects. *The Journal of Chemical Physics*, 137:204116, 2012.

[34] R. W. Baker. *Membrane Technology and Applications Third Edition*. Wiley, New York, 2012.

[35] C. Y. Tang, T. H. Chang, and A. G. Fane. Colloidal interactions and fouling of nf and ro membranes: A review. *Advances in Colloid and Interface Science*, 164:126–143, 2011.

[36] S. Shin, O. Shardt, P. B. Warren, and H. A. Stone. Membraneless water filtration using co2. *Nature Communications*, 8:15181, 2017.

[37] S. R. deGroot and P. Mazur. *Non-Equilibrium Thermodynamics*. North-Holland Publishing Co., Amsterdam, 1962.

[38] E.A. Guggenheim. *Thermodynamics*. North Holland, Amsterdam, 1967.

[39] R. P. A. Dullens, D. G. A. L. Aarts, and W. K. Kegel. Direct measurement of the free energy by optical microscopy. *Proceedings of the National Academy of Sciences of the United States of America*, 103:529–531, 2006.